International Journal of Advanced Science and Technology
Vol. 29, No. 2, (2020), pp. 3756 – 3765

Effect of modification on microstructure wear resistance and mechanical properties of Al-12.4%Si alloy

Dr. Israa . A. Alkadir
Department of Production Engineering and Metallurgy, University of Technology, Baghdad, Iraq, 70014@ uotechnology .edu.iq

Abstract

This work verifies the effect of adding different weight percentages of alloying elements boron and antimony 1,2 and 3 Wt% to Al-12.4% Si alloy by stir casting process on the wear rate, microstructure, and properties after the mechanical test. A microstructure was an inspection by optical microscopy of alloy before and after adding the additional elements. The examination represents that the change occurs on the size and morphology of α-Al, also refining the silicon in the eutectic phase. The results of the mechanical test showed that the hardness, yield strength, and tensile strength increased when the Wt% of alloying elements additions increasing, but the elongation decreases when we compared with the Al-12.4%Si alloy. The wear rate determined by the pin-on-disk device before and after alloying elements adding. Also, we observed that the wear rate decreased when increasing the Wt% of boron at different applied loads (5, 10, and15N) at a constant sliding speed (2.8) m/sec, and also at fixed applied load (15 N) with variance sliding velocity such as (1.4,2.8, and4.2M/sec).

Keywords: *Al-Si alloy, Alloying elements, Mechanical properties, Microstructure, Wear resistance*

Introduction

The Al-Si alloys are widely used in industrial applications, because of their best properties such as corrosion resistance, easy castability, good fluidity, low melting point, good machinability, and wear resistance. Silicon content and the morphology influence the properties at high and low temperatures. The silicon phase morphology can be modified by adding different alloying elements and by thermal treatments [1]. The aspects for changing Si –phase and eutectic are called modifiers, these modifiers such as Sb, Sn, Bi, Sr,Pb, Na, Ce, etc. The cast Al-Si alloy produced by melting, pouring and solidification. Properties of materials depend on the characteristics of its microstructure, modification and refinement are used for improving mechanical properties. There are different methods used for modifying and refinement by ultrasonic, squeeze, stirring, centrifugal, and vibration [1]. The transformation of eutectic silicon morphology in Al-Si cast alloys from the coarse plate-like to excellent fiber networks can be achieved by trace elements additions [2]. Xing et al. [3] studied the effect of the elements rare-earth on Al-Si alloys hypereutectic. The results showed the original silicon size is decreased very much with the suitable addition of RE on solidification of the Al-17.5 Si and Al-25Si alloys. After the RE addition to the Al-Si alloy, the changing occurs of the primary silicon to form a coarse shape to excellent facetted shape, changes in the distribution size of the primary silicon, and also improves the mechanical properties of the base alloys. Lina M. et al. [4] investigate the effect of manganese additions at different weight percent 0.1 to 0.5% and Cu content from 1.5 -7%dominate constituents. The results represent that the Mn addition to the base alloy, the tensile properties and hardness increased up to 0.6 % for the age and as-cast hardened conditions. Also, the addition of copper to alloy increased the tensile and hardness properties, but the impact energy decreased. Weixi SHI et al. [5] study the influence of neodymium on the primary silicon and mechanical properties of Al-15%Si alloy; the results show that the Nd addition 0.3% reduced the average size of primary silicon from 20-40 μm to 10-20μm of the modified sample. The results of mechanical properties showed that the tensile strength increased and elongated this due to the refinement of primary silicon.

Experimental Work

In this study, Al-Si alloy was used as the matrix material, antimony (Sb), and boron (B) used as alloying elements. Compositions of matrix alloy are shown in table (1).

Table .1. The chemical analysis of Al-Si alloy.

Alloy	Cu %	Mg%	Si %	Fe %	Mn %	Ni%	Zn %	Pb %	Ti %	Sb %	Al%
	0.05	0.04	12.4	0.33	0.24	0.032	0.23	0.1	0.03	-	Rem

A 300 gm for Al-Si alloy melted to 700^{o}C for 2hrs. Then the slag was removed by using calcium florid and argon gas. Antimony and boron added individually to molten alloy with different weight percentages 1, 2, and 3 wt%. The Sb and B elements after warped with aluminum foil, then after each addition of wrapped foil, the molten was stirred by using the preheated and coated plunger mild steel for 3-5 minutes at 400 rpm speed to enable complete homogenization and dissolution. Then the melt was poured into the preheated mold at 200^{o}C for 1 hrs. After casting, the cast was removed out of the mold. The casting, produced after the addition of B and Sb, was analyzed with an optical emission spectrometer (model: AMETEK the materials analysis DIVI- ION), as shown in table (2) and (3).

Table.2. Chemical composition of casting after alloying elements addition.

Sp.No	**Cu %**	**Mg%**	**Si%**	**Fe%**	**Mn %**	**Ni%**	**Zn%**	**Pb%**	**Ti%**	**Sb%**	**Al%**
1	0.05	0.04	12.4	0.33	0.24	0.032	0.23	0. 1	0.03	-	Rem
2	0.048	0.036	12.36	0.32	0.238	0.030	0.22	0.09	0.029	0.85	Rem
3	0.047	0.037	12.34	0.31	0.237	0.029	0.21	0.089	0.028	1.85	Rem
4	0.046	0.0365	12.35	0.299	0.236	0.0285	0.20	0.088	0.025	2.86	Rem

Table.3. The chemical composition of casting after addition alloying elements.

Sp.No	**Cu %**	**Mg%**	**Si%**	**Fe%**	**Mn %**	**Ni%**	**Zn%**	**Pb%**	**Ti%**	**B %**	**Al%**
1	0.05	0.04	12.4	0.33	0.24	0.032	0.23	0. 1	0.03	-	Rem
2	0.046	0.038	12.37	0.32	0.236	0.030	0.22	0.084	0.028	0.87	Rem
3	0.048	0.037	12.34	0.31	0.237	0.029	0.21	0.086	0.025	1.9	Rem
4	0.049	0.0365	12.32	0.299	0.239	0.0285	0.20	0.087	0.027	2.89	Rem

The shape of the specimens was cylindrical with10 mm height and 20 mm in diameter. The specimens were prepared by using a grinding machine (model: MOPAO 160E) and paper of silicon carbide grades (120, 500, and 1000), respectively, under the running tap waters. Then samples were polished by the machine model (UNIPOL 820) with (2μm) and with 0.5μm Al_2O_3 slurry. Finally, etching the

specimens with Killer's solution, which contains different amounts of acids (1.5 ml HCl +1 ml HF+ 2.5 ml HNO3 +95 ml distilled water).

The microstructures of prepared alloy before and after adding different weight percentages of B and Sb were examined under the optical computerized microscope model (BEL metallographic engineering microscopes). The hardness value of all samples was calculated after testing by the Vickers hardness machine. Tensile tests were carried out by a computer-controlled electronic universal testing machine (Model: WDW-100) with a crosshead speed of 1mm/min. Figure. (1) Shows the tensile test standard specimen with ASTM standard E8M – 00b [6]. A steel disc with 35 HRC hardness used as a counter face. The disc rotational speed was (490 RPM), the loads utilized were 5, 10, and 15 N and with different velocity 1.4, 2.8, and 4.2 m/sec and time 30 min. The specimens were prepared for wear test with 10 mm in diameter, and 20mm high was cut from cast samples.

The linear speed was calculated as follows: -

$$V = \frac{\pi D s N}{1000 \times 60} \quad - - (1)$$

Where: -

V= Sliding velocity (m/sec)

Ds=Sliding circle diameter.

N=Rotational speed of disc (490) RPM

The following equation used to calculate the wear rate: -

$$\text{Wear rate (weight loss)} = \frac{\Delta w}{s} \ (\text{m/cm}) - \quad (2)$$

Where:

ΔW= The weight loss of sample (gm)

W_1= The weight of the sample before the wear test (gm).

W_2= The weight of the sample after the wear test (gm).

The sliding distance (S) in cm was determined as: -

$$S = V \times t \qquad (3)$$

Where: -

t=Sliding time (30 min) at each test

The Results and Discussion

1-Microstructural Observation

The microstructure of non modified Al-12.4% Si alloy appears in Figure (2) it generally observed coarse dendritic α-Al and eutectic Si structure this phenomenon could be seen by optical microscope. The effect of boron and antimony additions on microstructure shown in Figure (3) a, b, c, d,e, and f. The change in the morphology of α-Al and eutectic silicon structure, the Si –particles from plate-like to fibrous, is achieved. There are two essential mechanisms of the modification process operating. The first, the nuclei of eutectic silicon in the molten alloy are removed by modification alloying elements based on the phenomenon of nucleation undercooling increased; also, the eutectic solid-liquid interface advances at the higher rate of growth. The second, interface of a eutectic silicon structure, the phase –liquid changed by the modification elements depends on the observation of high growing twins density, which transformation the manner of eutectic silicon growth. The cells of eutectic are refined into a fully eutectic modified microstructure [8].

2-Tensile Properties

The Figure (4) and (5) represent that the ultimate tensile strength and yield strength increases with increasing the weight percentage of alloying elements when adding boron element the result gives

higher values of the ultimate tensile strength and yield strength when compared with Sb addition and the base alloy, but the elongation decreases as shown in Figure (6). This is because the alloying elements modifying the α-Al and refining the eutectic Si structure this increases in Al-Si interface and hindering the movement of dislocations .A ccording to Hall –Petch[9] equations which described the increase in the tensile strength as the following:-

$\sigma = \sigma_o + Kd^{\wedge -1/2}$ -------4

3-Hardness Test

The size, morphology, and distribution of the Si-particles affect the hardness of the eutectic matrix. Figure (7) represents that the hardness increased with increasing the weight percentage of B and Sb additions. This is due to the modification of α-Al and changing the Si structure in the eutectic matrix of Al-Si alloy. The changing in shape, size, and morphology of the α-Al and Si phase also expected that producing the intermetallic compounds such as AlSi, AlSiSb, and AlSiB leads to increasing hardness[10].

4-Wear Test

In this research, three loads were used (5,10, and 15 N), to study the influence of applied loads on wear rate under the constant sliding speed of 2.8 m/sec and at 30 min. Figures(8) and (9) demonstrated that the rate of wear generally increases with the normally applied loads increased. As the load increased, the wear rate also increases because of plastic deformation increasing at the tip of the sample surface sprites between sliding surface increase, which causes the sliding surface adhesion between surface asperities where depends on the amount and the value of average load applied. If the applied load is small, therefore a weak contact occurs at the tip of surface asperities only [10]. When the sliding process appears, the low contact occurs, which represents the thin oxide layer thus acts as a protective film of oxide on the surface that covers the sliding surface and also direct protects of the metal in which the contact occurs between the surface of asperities. The force required to shear and separate the connection between the asperities of the surface when occurs the lower bonding force between the atoms of metal and also a lower wear rate will produce. When it increases the applied load, the fracture of the surface oxide layer will occur because the brittleness of it will be extruded outside the sliding surface of the specimen and disc through out the sliding process. This produces a metallic junction to each other. The shear force required to shear the connected asperities is higher than the bonding force between metal atoms themselves; therefore, it will lead to separation of the metallic particles from the metal surface and finally increase in the wear rate. The wear resistance increased with increasing the weight percentage of alloying elements additions because of increasing hardness due to modification of eutectic silicon and α-Al, and increasing the distortion in the crystal structure and dislocations density[10]. Figures (10) and (11) represent the influence of different sliding velocity (1.4, 2.8, and 4.2) m/ sec at constant applied load and time, respectively 10 N and 30min. The wear rate decreases with increasing the sliding velocity. This is because of the increase in the flash temperature produced by sliding of the contact surface between each other with increasing sliding speed. The flow of heat through the specimen metal at higher sliding speed is lower than that at lower sliding speed. This will lead to the softening of specimen surface asperities at the low sliding speed, which produces partial welding between the sliding surface asperities. The required force to shear contact points is higher than the bonding force of the atomic itself. Therefore the wear rate increases with decreasing sliding speed[12,13]. Also, the results observed that the alloy pin, which contains 3Wt% B, has a lower wear rate when compared with adding Sb and with the base alloy.

5-Conclusions

The addition of alloying elements B and Sb modified the α-Al phase and silicon in the eutectic matrix alloy. Refining the grain size α-Al phase by increasing the weight percentage of B when compared with Sb. Tensile strength and yield stress increased with the weight percent of adding alloying elements, but the elongation decreases when compared with the base alloy. Addition of 3Wt% B gives higher hardness when compared with Sb adding and base alloy. Rate of wear decreases with increasing the weight percentage of B and Sb compared with the base alloy. The wear rate decreases when adding alloying elements Sb and B with increasing load and sliding speed compared with base alloy.

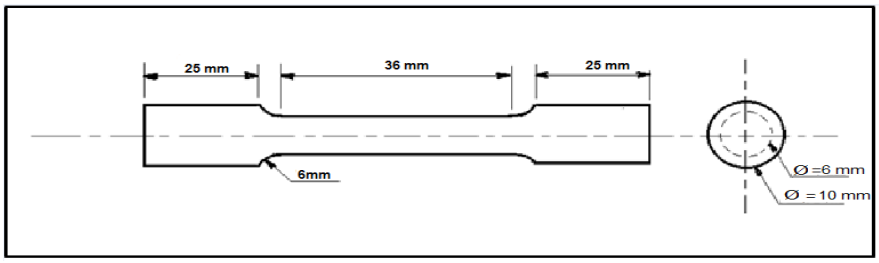

Figure .1. Standard tensile test specimen [6].

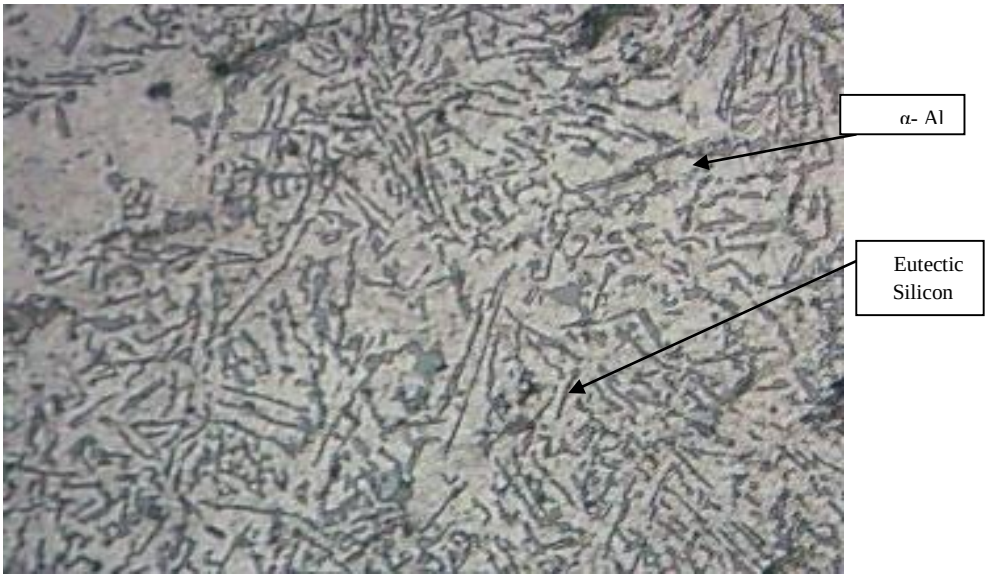

Figure.2. Optical Micrograph of Al-12.4%Si alloy.Mag.125X

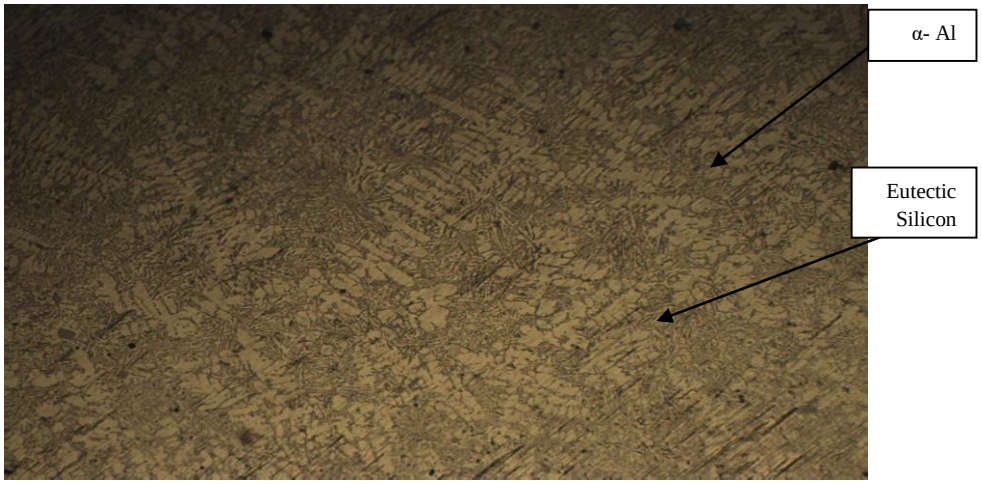

a- 1Wt% Boron

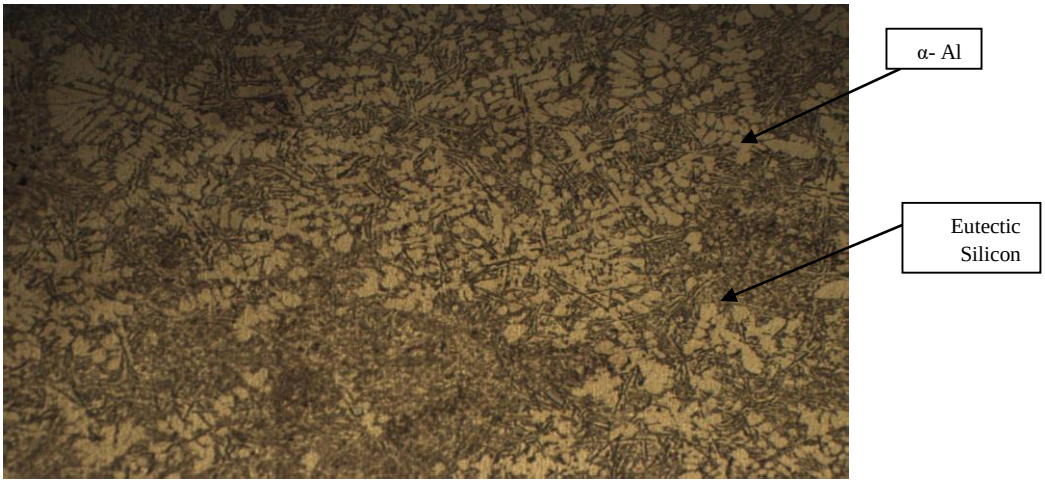

b-2Wt% Boron

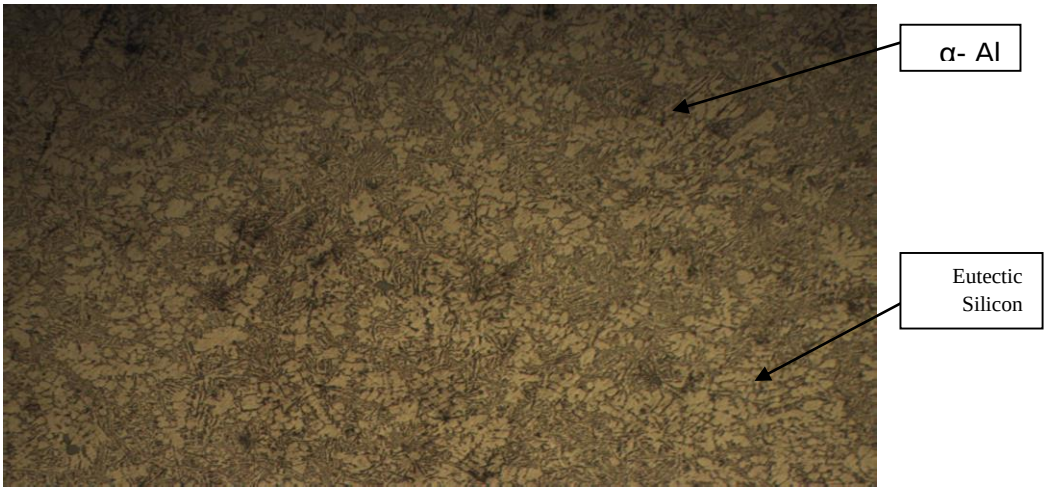

-3 Wt% Boron c

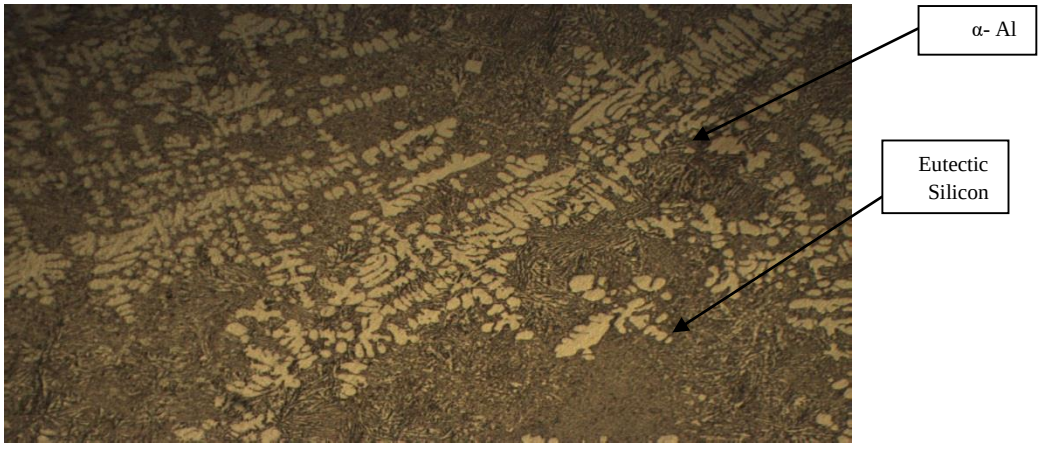

d-1Wt% Antimony

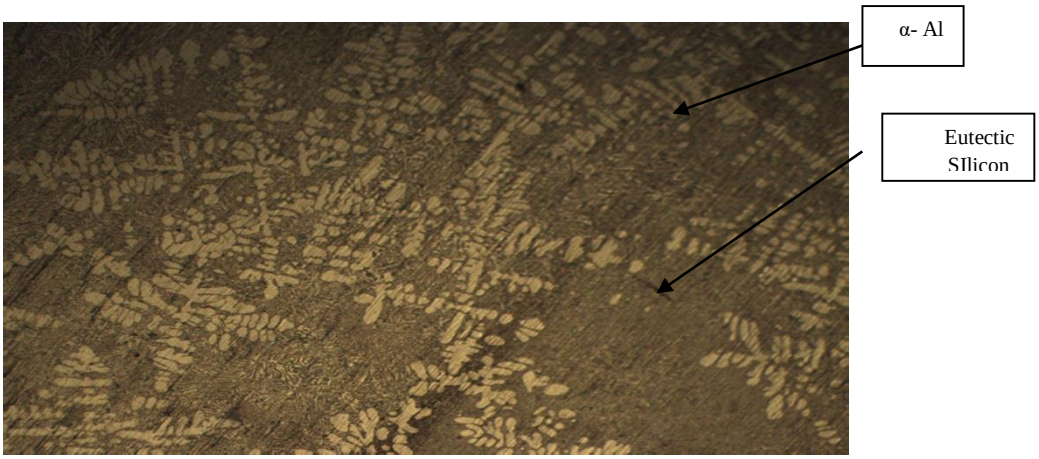

e-2Wt%Antimony

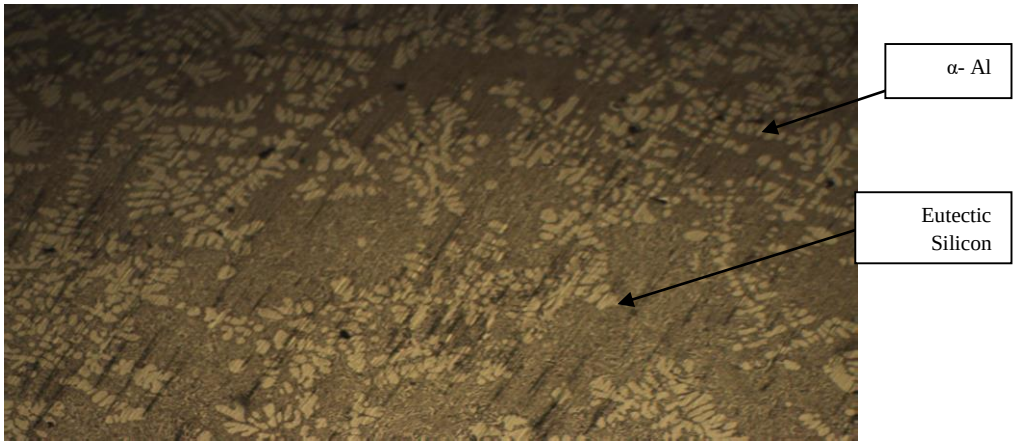

F- 3 Wt% Antimony.

Figure.3. Optical micrographs of Al-12.4%Si after adding alloying elements.Mag.100X

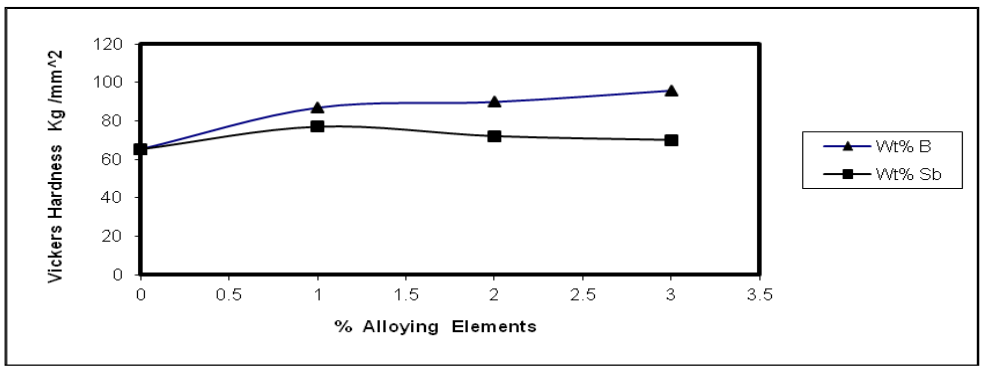

Figure .4. The relation between the weight percentage of alloying elements and hardness.

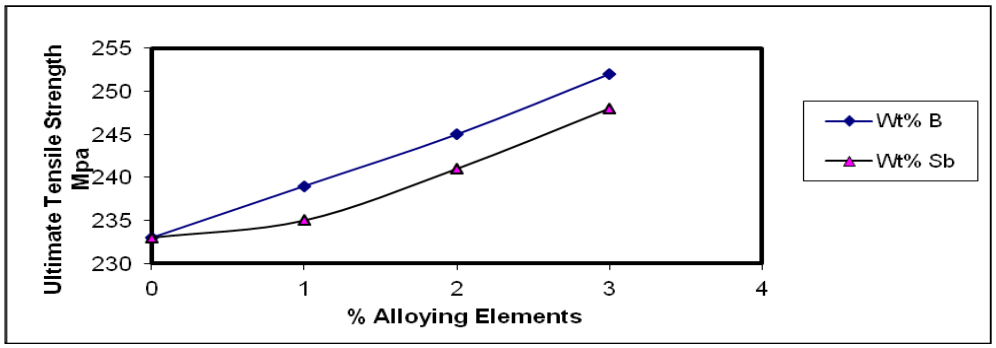

Figure.5. The relation between ultimate tensile strength and weight percentage of alloying elements.

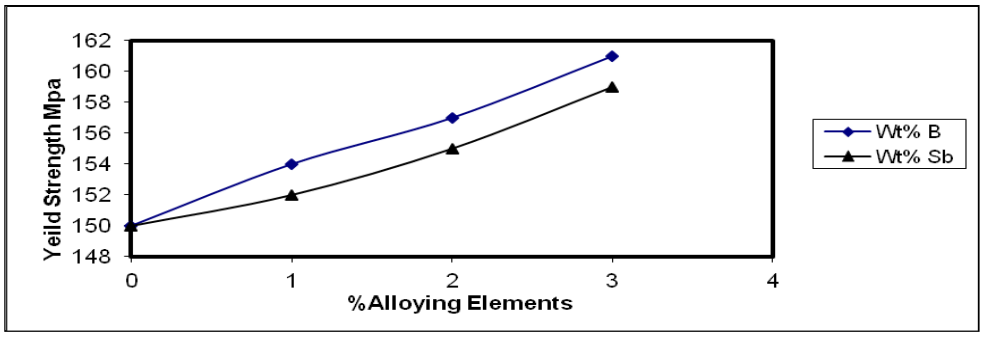

Figure.6. The relation between the weight percentage of alloying elements and elongation.

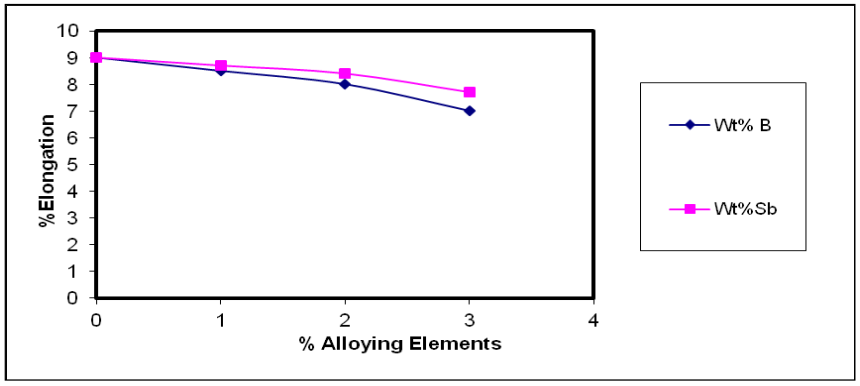

Figure.7. The relation between the weight percentage of alloying elements and elongation.

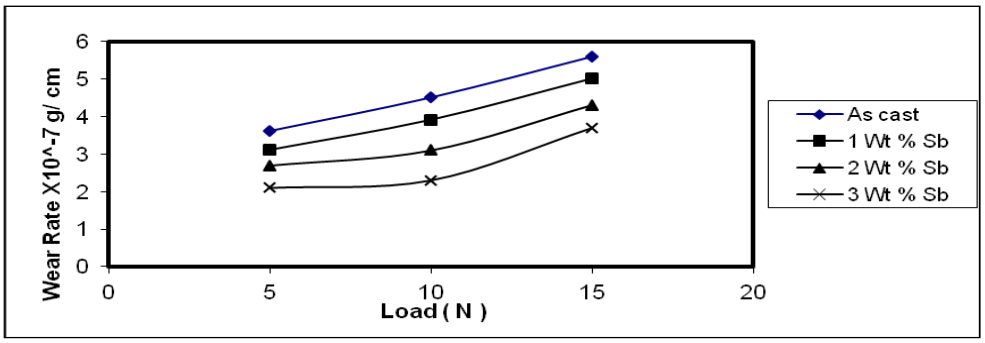

Figure.8. The relation between load and wear rate at a constant sliding speed of 2.8 m/sec.

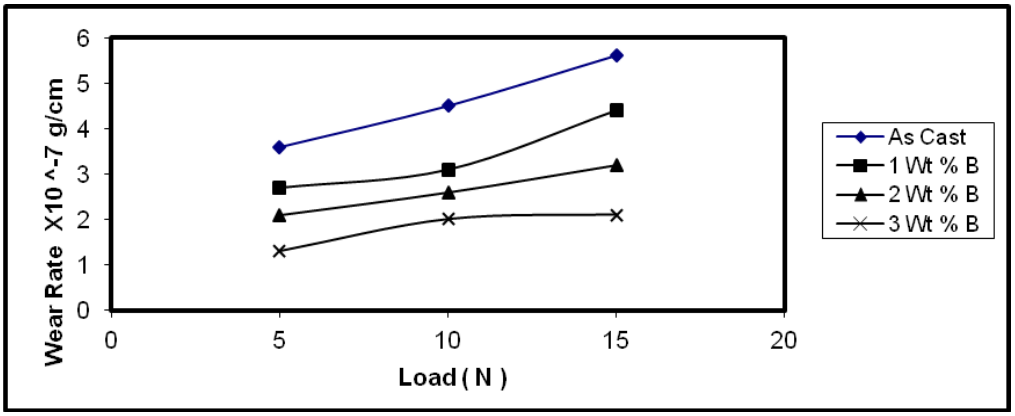

Figure .9. The relation between load and wear rate at a constant sliding speed of 2.8 m/sec.

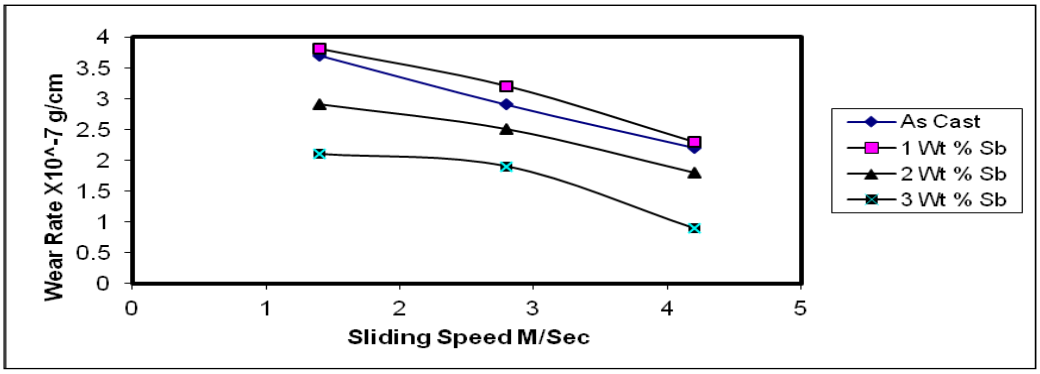

Figure.10. The relation between sliding speed and wear rate at a constant load of 10 N.

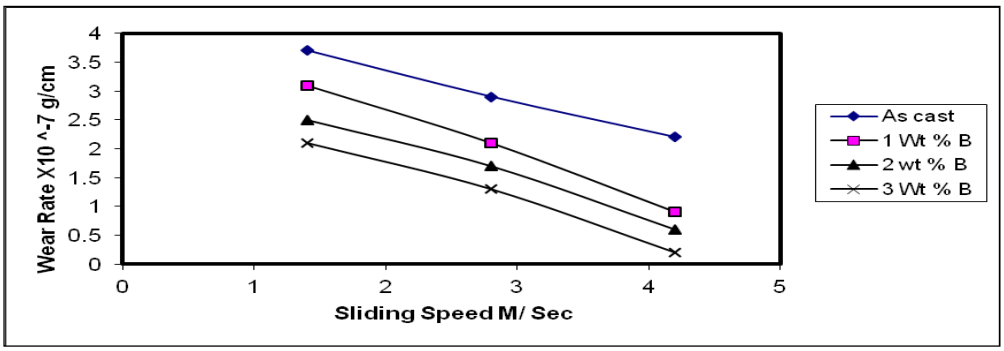

Figure.11. The relation between sliding speed and wear rate at a constant load of 10 N.

References

1. Mohamed.H. A, Agnes .M.S, Herbert. W. Doty, Salvador .V, and Fawzy .H.S," Effect of additives on the microstructure and tensile properties of Al-Si alloys," Journal of material research and technology, Vol,8, Issue 2, 2019, PP, 2255.
2. Toni. B, Arne. K. D, and Salem. S, "Effect of Co and Ni addition on the microstructure and mechanical properties at room and elevated temperature of an Al-7%Si alloy. International journal of metal casting, Vol.12, Issue 3, PP.434.
3. Xing, P., B, Zhuang, Y, and Liu, K, "On the modification of hypereutectic Al-Si alloys using rare earth Er," Acta Metall, Vol, 23, No,5,2010, PP, 327.

4. Lina M.Shehadeh, Issam S.Jaiham, " The effect of adding different percentages of Mn and Cu on the mechanical behavior of Al," Jourdan Journal of Mechanical and Industrial Engineering, Vol.10, No.1,2016, PP.19-26.
5. Weixi SHI, Bo GAO, Ganfeng TU, Shiwei LI, YiHAO, and Fuxiao YU," Effect of neodymium on first silicon and mechanical properties of hypereutectic Al-15%Si alloy, Journal of rare piles of earth, Vol 28, No, 1,2010, PP367-370.
6. Standard Test Method for Tension Testing of Metallic Material, American Association State, Highway and Transportation Officials Standard, AASHTO No: T68, An American National; Standard.
7. Aiqin. W, Lijun .Z, and Jingpei.Xie, "Effect of Cerium and Phosphorus on microstructures and properties of hypereutectic Al-21%Si alloy, Journal of rare piles of earth, Vol.31, Issue 5, 2013, PP.522.
8. Chunjie G, Hao Tu, and Xuping Su," Study on microstructure and mechanical properties of hypereutectic Al-18Si alloy modified with A-3B ", journal Materails, Vol.11, No. 3, 2018, PP.456.
9. Saha S, Tareq SH, and Galib RH, "Effect of over aging conditions on microstructure and mechanical properties in Al-Si –Mg alloy, "Journal of material science and engineering, Vol.5, No.5, 2016, PP.1-4
10. Mohamed H, Agnes M.S, Herbert W, Salvador V, and Fawzy H," Effect of additives on the microstructure and tensile properties of Al-Si alloys," Journal of materials research and technology" Vol 8, Issue 2, 2019, PP.2255-2268.
11. Clarke and A.D. Sarkar, Wear characterization of as-cast binary aluminum-silicon alloys, Wear, 54 (1979) 7-16.
12. Wu X.F. and Zhang G. A, Influence of Sn content on the microstructure and dry sliding wear behavior of hypereutectic Al-20Si alloy, J. Mat Sci. 46 (2011) 7319-7327.
13. Lozano D.E, Mercado R.D, and Perez a.J, Tribo-logical behavior of cast hypereutectic Al-Si-Cu alloy subjected to sliding wear, Wear 297 (2009) 545-549.